Determination of the math xmlns="http://www.w3.org/1998/Math/MathML" display="inline">mrow>mmultiscripts>mrow>mi>Al/mi>/mrow>mprescripts>/mprescripts>none>/none>mrow>mn>27/mn>/mrow>/mmultiscripts>/mrow>/math> Neutron Distribution Radius from a Parity-Violating Electron Scattering Measurement

D. Androić et al. (math xmlns="http://www.w3.org/1998/Math/MathML" display="inline">mrow>msub>mrow>mi mathvariant="normal">Q/mi>/mrow>mrow>mrow>mi>weak/mi>/mrow>/mrow>/msub>/mrow>/math> Collaboration)

Phys. Rev. Lett. **128**, 132501 — Published 1 April 2022

DOI: 10.1103/PhysRevLett.128.132501

First Determination of the ^{27}Al Neutron Distribution Radius from a Parity-Violating Electron Scattering Measurement

D. Androić,[1] D.S. Armstrong,[2,*] K. Bartlett,[2] R.S. Beminiwattha,[3] J. Benesch,[4] F. Benmokhtar,[5] J. Birchall,[6] R.D. Carlini,[4,2] J.C. Cornejo,[2] S. Covrig Dusa,[4] M.M. Dalton,[7,4] C.A. Davis,[8] W. Deconinck,[2] J.F. Dowd,[2] J.A. Dunne,[9] D. Dutta,[9] W.S. Duvall,[10] M. Elaasar,[11] W.R. Falk,[6,†] J.M. Finn,[2,†] T. Forest,[12,13] C. Gal,[7] D. Gaskell,[4] M.T.W. Gericke,[6] V.M. Gray,[2] K. Grimm,[13,2] F. Guo,[14] J.R. Hoskins,[2] D.C. Jones,[7] M.K. Jones,[4] M. Kargiantoulakis,[7] P.M. King,[3] E. Korkmaz,[15] S. Kowalski,[14] J. Leacock,[10] J. Leckey,[2] A.R. Lee,[10] J.H. Lee,[2,3] L. Lee,[8,6] S. MacEwan,[6] D. Mack,[4] J.A. Magee,[2] R. Mahurin,[6] J. Mammei,[10,6] J.W. Martin,[16] M.J. McHugh,[17] D. Meekins,[4] K.E. Mesick,[17,18] R. Michaels,[4] A. Micherdzinska,[17] A. Mkrtchyan,[19] H. Mkrtchyan,[19] A. Narayan,[9] L.Z. Ndukum,[9] V. Nelyubin,[7] Nuruzzaman,[20,9] W.T.H van Oers,[8,6] V.F. Owen,[2] S.A. Page,[6] J. Pan,[6] K.D. Paschke,[7] S.K. Phillips,[21] M.L. Pitt,[10] R.W. Radloff,[3] J.F. Rajotte,[14] W.D. Ramsay,[8,6] J. Roche,[3] B. Sawatzky,[4] T. Seva,[1] M.H. Shabestari,[9] R. Silwal,[22] N. Simicevic,[13] G.R. Smith,[4,‡] P. Solvignon,[4,†] D.T. Spayde,[23] A. Subedi,[9] R. Suleiman,[4] V. Tadevosyan,[19] W.A. Tobias,[7] V. Tvaskis,[16,6] B. Waidyawansa,[3] P. Wang,[6] S.P. Wells,[13] S.A. Wood,[4] S. Yang,[2] P. Zang,[24] and S. Zhamkochyan[19]

($Q_{\rm weak}$ Collaboration)

M.E. Christy,[20] C.J Horowitz,[25] F.J. Fattoyev,[25,§] and Z. Lin[25,¶]

[1] *University of Zagreb, Zagreb, HR 10002, Croatia*
[2] *William & Mary, Williamsburg, Virginia 23185, USA*
[3] *Ohio University, Athens, Ohio 45701, USA*
[4] *Thomas Jefferson National Accelerator Facility, Newport News, Virginia 23606, USA*
[5] *Christopher Newport University, Newport News, Virginia 23606, USA*
[6] *University of Manitoba, Winnipeg, Manitoba R3T2N2, Canada*
[7] *University of Virginia, Charlottesville, Virginia 22903, USA*
[8] *TRIUMF, Vancouver, British Columbia V6T2A3, Canada*
[9] *Mississippi State University, Mississippi State, Mississippi 39762, USA*
[10] *Virginia Polytechnic Institute & State University, Blacksburg, Virginia 24061, USA*
[11] *Southern University at New Orleans, New Orleans, Louisiana 70126, USA*
[12] *Idaho State University, Pocatello, Idaho 83209, USA*
[13] *Louisiana Tech University, Ruston, Louisiana 71272, USA*
[14] *Massachusetts Institute of Technology, Cambridge, Massachusetts 02139, USA*
[15] *University of Northern British Columbia, Prince George, British Columbia V2N4Z9, Canada*
[16] *University of Winnipeg, Winnipeg, Manitoba R3B2E9, Canada*
[17] *George Washington University, Washington, DC 20052, USA*
[18] *Rutgers, The State University of New Jersey, Piscataway, New Jersey 08854, USA*
[19] *A. I. Alikhanyan National Science Laboratory (Yerevan Physics Institute), Yerevan 0036, Armenia*
[20] *Hampton University, Hampton, Virginia 23668, USA*
[21] *University of New Hampshire, Durham, New Hampshire 03824, USA*
[22] *University of Virginia, Charlottesville, VA 22903, USA*
[23] *Hendrix College, Conway, Arkansas 72032, USA*
[24] *Syracuse University, Syracuse, New York 13244, USA*
[25] *Indiana University, Bloomington, Indiana 47405, USA*

We report the first measurement of the parity-violating elastic electron scattering asymmetry on ^{27}Al. The ^{27}Al elastic asymmetry is $A_{\rm PV} = 2.16 \pm 0.11$ (stat) $\pm$ 0.16 (syst) ppm, and was measured at $\langle Q^2 \rangle = 0.02357 \pm 0.00010$ GeV^2, $\langle \theta_{\rm lab} \rangle = 7.61^\circ \pm 0.02^\circ$, and $\langle E_{\rm lab} \rangle = 1.157$ GeV with the $Q_{\rm weak}$ apparatus at Jefferson Lab. Predictions using a simple Born approximation as well as more sophisticated distorted-wave calculations are in good agreement with this result. From this asymmetry the ^{27}Al neutron radius $R_n = 2.89 \pm 0.12$ fm was determined using a many-models correlation technique. The corresponding neutron skin thickness $R_n - R_p = -0.04 \pm 0.12$ fm is small, as expected for a light nucleus with a neutron excess of only 1. This result thus serves as a successful benchmark for electroweak determinations of neutron radii on heavier nuclei. A tree-level approach was used to extract the ^{27}Al weak radius $R_{\rm w} = 3.00 \pm 0.15$ fm, and the weak skin thickness $R_{\rm wk} - R_{\rm ch} = -0.04 \pm 0.15$ fm. The weak form factor at this Q^2 is $F_{\rm wk} = 0.39 \pm 0.04$.

As beam properties and experimental techniques have improved over the last two decades, so has the precision of parity-violating (PV) asymmetry measurements in elastic electron scattering. These experiments initially focused on carbon [1], then hydrogen and helium targets to study strange quark form factors [2]. The improving precision of these experiments has led to standard model tests [3, 4], and even more recently neutron radius determinations in heavy nuclei [5, 6] which impact our understanding of the structure and composition of neutron stars [7].

The proton's weak charge was determined in the $Q_{\rm weak}$ experiment [4, 8] by measuring the PV asymmetry in $\vec{e}p$ elastic scattering with high precision at low Q^2. By far the largest background in that experiment ($\approx 24\%$) came from the aluminum alloy cell that contained the hydrogen. To accurately account for that background, precise additional asymmetry measurements were made on aluminum interspersed between data taking on hydrogen.

Those same aluminum asymmetry results that served to account for background in the $Q_{\rm weak}$ experiment have been further analyzed in this work to isolate the ^{27}Al asymmetry $A_{\rm PV}$ for elastic electron scattering at $Q^2 = 0.02357$ GeV^2. A successful comparison with theory [9] would provide additional confidence in the empirical background subtraction used in the $Q_{\rm weak}$ experiment [4].

However, the most important aspect of the first ^{27}Al $A_{\rm PV}$ measurement presented here is the test case it provides for the electroweak (EW) technique [10] used to determine the neutron radius R_n of a complex nucleus in $\vec{e}A$ scattering. In conjunction with the more easily-determined proton radius R_p, this also delivers the neutron skin $R_n - R_p$.

For a light complex nucleus like ^{27}Al with a neutron excess of only 1, we expect the neutron skin to be very thin. If this naïve expectation is confirmed by our measurement, it would serve as a benchmark for the application of the EW technique to heavier nuclei like ^{208}Pb, where the resulting neutron skin can be related to neutron star physics [7]. The EW technique has recently been applied to ^{208}Pb [5] and the resulting neutron skin was found to be in some tension with earlier non-EW results [11, 12] which favor a thinner skin. The benchmark of the EW technique which our result can provide is especially important in light of this observed tension.

Beyond providing the ^{27}Al asymmetry $A_{\rm PV}$, neutron radius R_n, and neutron skin thickness $R_n - R_p$, we also report the ^{27}Al weak form factor $F_{\rm wk}$ at our Q^2, the ^{27}Al weak radius $R_{\rm wk}$ and weak skin thickness $R_{\rm wk} - R_{\rm ch}$, where $R_{\rm ch}$ is the charge radius. $R_{\rm wk}$ should closely track the neutron radius because the weak charge comes primarily from the neutrons – the proton's weak charge is much smaller [4].

A PV asymmetry is a non-zero difference between differential cross sections $\sigma_\pm(\theta)$ measured with a beam polarized parallel $(+)$ or anti-parallel $(-)$ to its incident momentum. In the Born approximation the elastic $\vec{e}$–^{27}Al asymmetry can be expressed [9] as

$$A_{\rm PV} = \frac{\sigma_+(\theta) - \sigma_-(\theta)}{\sigma_+(\theta) + \sigma_-(\theta)} \approx \frac{-G_F Q^2 Q_W}{4\pi\alpha Z\sqrt{2}} \frac{F_{\rm W}(Q^2)}{F_{\rm EM}(Q^2)}, \quad (1)$$

where G_F is the Fermi constant, α is the fine structure constant, $-Q^2$ is the four-momentum transfer squared, $Q_W = -12.92 \pm 0.01$ is the predicted [13] weak charge of ^{27}Al including all radiative corrections, and Z is the atomic number of ^{27}Al. $F_{\rm W}(Q^2)$ and $F_{\rm EM}(Q^2)$ are the weak and electromagnetic (EM) form factors for ^{27}Al, normalized to unity at $Q^2 = 0$.

This measurement was conducted in Hall C of Jefferson Lab using the $Q_{\rm weak}$ experimental apparatus [14] and the polarized electron beam of the CEBAF accelerator. The helicity of the polarized electron beam was selected at a rate of 960 Hz, allowing the beam to be produced in a sequence of "helicity quartets", either $(+--+)$ or $(-++-)$, with the pattern chosen pseudorandomly at 240 Hz. In addition, every 8 hours an insertable half-wave plate (IHWP) was placed in or out of the source laser's path to reverse the polarization direction. A 'double Wien' spin rotator was also used to reverse the electron spin direction twice during the ^{27}Al data-taking.

A 60 μA longitudinally polarized 1.16 GeV electron beam was incident on a 3.68 mm thick by 2.54 cm square 7075-T651 aluminum alloy target. This target was machined from the same lot of material used for the LH_2 target window components of the weak charge measurement, so it could also be used to account for the background aluminum asymmetry that contaminated the measured hydrogen asymmetry [3, 4]. Other elements in this alloy, as determined during a post-experiment assay, include: Zn (5.87 wt%), Mg (2.63 wt%), Cu (1.81 wt%), and other (0.47 wt%).

Electrons scattered from the target were first selected by a series of three collimators and were then focused by a toroidal magnetic field onto an azimuthally-symmetric array of eight synthetic-quartz Cherenkov detectors, each with a 2-cm-thick lead preradiator. The polar-angle (θ) acceptance was 5.8° to 11.6°, the azimuthal-angle acceptance was 49% of 2π, and the energy acceptance was large: $\approx$ 150 MeV. Cherenkov light generated in the quartz from the passing electrons was collected by photomultiplier tubes (PMTs) attached to each end of each detector in the array. The current from the PMTs was integrated over each helicity state, normalized to the beam current and then averaged together to form the raw asymmetry $A_{\rm raw}$, as shown in Fig. 1 and Tab. I. Several small systematic corrections were applied to $A_{\rm raw}$ to derive a measured asymmetry $A_{\rm msr}$:

$$A_{\rm msr} = A_{\rm raw} + A_{\rm BCM} + A_{\rm reg} + A_{\rm BB} + A_{\rm L} + A_{\rm T} + A_{\rm bias}, \quad (2)$$

where $A_{\rm BCM}$ is a beam-current monitor (BCM) normalization uncertainty, $A_{\rm reg}$ is a helicity-correlated beam-motion correction, $A_{\rm BB}$ is a beam-line background correction, $A_{\rm L}$ is a non-linearity correction, $A_{\rm T}$ is a residual

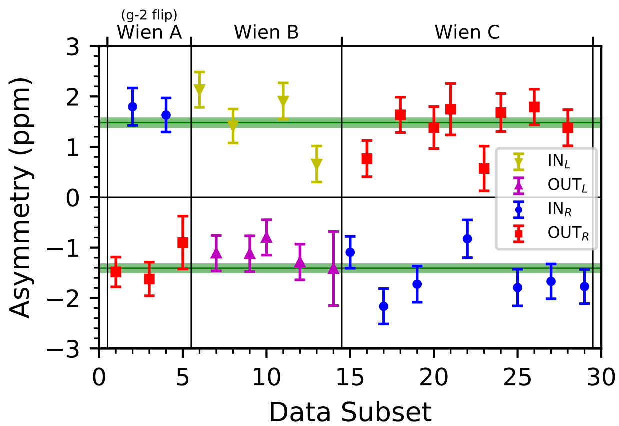

FIG. 1. Raw asymmetries (statistical errors only) plotted against 8-hour IHWP IN or OUT "data subsets" (lower axis), and monthly L or R Wien spin rotator orientation (upper axis). The configuration consistent with Eq. 1 is given by Wien Left and IHWP IN, i.e. IN_L, which is equivalent to OUT_R. The opposite sign asymmetry arises when either the Wien or the IHWP is flipped, but not both. During Wien A, there was an additional $(g-2)$ spin flip which arose from running the JLab recirculating linac with 2 passes at half the gradient instead of 1 pass with full gradient. The green lines (bands) denote weighted averages (uncertainties) of the positive and negative asymmetries.

TABLE I. Time-averaged raw asymmetries and their statistical uncertainties. A_{raw} is the weighted average of the sign-corrected raw asymmetries NEG and POS. NULL is the arithmetic average of NEG and POS. The χ^2 per degree of freedom and associated probabilities are given for each type of average.

Average	Asymmetry(ppm)	$\chi^2/d.o.f.$	χ^2 Prob.
NEG	-1.407 $\pm$ 0.093	1.26	0.225
POS	1.480 $\pm$ 0.099	1.62	0.073
NULL	0.036 $\pm$ 0.068	–	–
A_{raw}	1.441 $\pm$ 0.068	1.39	0.082

transverse-asymmetry correction, and A_{bias} is a rescattering bias correction. Each of these corrections is discussed below.

The raw asymmetry charge normalization adopted the same technique and BCMs as used in the weak charge measurement [4], leading to a correction of $A_{\mathrm{BCM}} = 0.0 \pm 2.1$ ppb, dominated by the BCM accuracy.

Helicity-correlated variations in the beam position and energy also required a correction $A_{\mathrm{reg}} = 0.4 \pm 1.4$ ppb. This was determined with a linear regression method [3, 15], to correct the effects of natural beam-motion using helicity-correlated differences measured with different beam-position monitors.

Electrons in the beam halo interacted with beam-line components causing a false asymmetry. Auxiliary detectors placed close to the beam line were used to form a correlation with the main detectors to correct for this false asymmetry. The overall correction was $A_{\mathrm{BB}} = -4.7 \pm 6.6$ ppb.

Non-linearity effects in the main detector PMTs and BCMs used for asymmetry normalization were quantified in bench-top tests. The correction for this effect was $A_{\mathrm{L}} = -2.0 \pm 7.0$ ppb [15, 16].

Any residual transverse components to the beam polarization will cause a parity-conserving azimuthal variation in the asymmetry, which coupled with imperfections in the azimuthal symmetry of the detectors may lead to a false asymmetry. This was measured using transversely polarized beam [17] and scaled to the measured azimuthal variation in the present data, leading to a correction $A_{\mathrm{T}} = -3.4 \pm 8.8$ ppb [15].

As described in earlier publications [4, 8], lead preradiators placed in front of the main detectors were needed to reduce low-energy backgrounds. However, scattered electrons with spins precessing from longitudinal to transverse in the spectrometer magnetic field acquired an analyzing power from Mott scattering in the lead, which led to a correction of $A_{\mathrm{bias}} = 4.3 \pm 3.0$ ppb.

Determination of a purely elastic asymmetry A_{PV} required additional corrections for beam polarization, background asymmetries, and a combination of radiative and acceptance corrections:

$$A_{\mathrm{PV}} = R_{\mathrm{tot}} \frac{A_{\mathrm{msr}}/P - \sum_i f_i A_i}{1 - \sum_i f_i}, \tag{3}$$

where $R_{\mathrm{tot}} = 0.9855 \pm 0.0087$, determined primarily by simulation [4], accounts for the radiative and finite acceptance effects, f_i is the signal fraction of a particular background asymmetry, and A_i is its corresponding asymmetry. These can be found in Tab. II.

The beam polarization was monitored continuously using a Compton polarimeter [18] and periodically with dedicated measurements using a Møller polarimeter [19]. Both were found to agree [20] during the experiment and yielded a combined polarization of $P = 88.80 \pm 0.55\%$.

Non-elastically scattered electrons entering the large acceptance of the apparatus contaminated the measured asymmetry with backgrounds which had to be estimated and subtracted in Eq. 3. Non-elastic processes considered in this analysis include quasi-elastic, single-particle and collective excitations, and inelastic scattering with a Δ in the final state. Correction for each of these backgrounds required knowledge of the fraction of events that fell into the acceptance, f_i, derived from the cross section of each process at the kinematics of the experiment, and A_i, the asymmetry for each process. Both of these were determined using models and/or experimental data from previous measurements. The relevant dilutions for each of these background processes were reported in [17].

The quasi-elastic asymmetry A_{QE} was estimated for ^{27}Al from a relativistic Fermi gas model [21], with a conservative 50% relative uncertainty.

The inelastic asymmetry $A_{\rm inel}$ was determined by dropping the spectrometer magnetic field to about 75% of its nominal value to move the inelastic events onto the detectors. The corresponding polarization-corrected ^{27}Al asymmetry

$$A^{75} = f^{75}_{\rm el} A^{75}_{\rm el} + f^{75}_{\rm inel} A^{75}_{\rm inel} = 1.36 \pm 0.97 \text{ ppm} \quad (4)$$

was briefly measured, with $f^{75}_{\rm inel}$ estimated from simulation to be $(20 \pm 5)\%$ on top of the elastic tail, and $A^{75}_{\rm el}$ scaled down from its value at full field by 1.181, the ratio of the corresponding Q^2 at each field. A value for $A_{\rm inel} = -0.58 \pm 5.83$ ppm at full field was obtained by solving Eq. 4 for $A^{75}_{\rm inel}$ and then scaling up by the Q^2 ratio.

Following the work of [9], the asymmetry for the giant dipole resonance was estimated using the Born approximation for an $N = Z$ nucleus, with a negative sign $A_{\rm GDR} = -2.2 \pm 1.1$ ppm appropriate for this isovector transition, and a conservative 50% relative uncertainty.

Asymmetries $A_{\rm nucl} \approx 2.5$ ppm for the 11 strongest excited states of ^{27}Al up to 7.477 MeV were also obtained using the Born approximation for elastic scattering, with small corrections made for the acceptance-averaged Q^2. States with large E2 transition rates or which were strongly populated by $T = 0$ probes were assumed to be isoscalar and assigned 50% uncertainties. The remaining states were assumed to be isovector. Since the sign of the asymmetry depends on whether those isovector states were proton or neutron excitations, a 200% uncertainty was used to encompass both possibilities.

For the asymmetries $A_{\rm alloy}$ associated with the contaminant elements in the alloy used for the target, the Born approximation calculation was again used as described in [9] for each of the dominant six elements. These calculations include Coulomb distortions, but assume spherically symmetric proton and neutron distributions, so only include the leading multipole term. As before, 50% uncertainties were used.

Background contributions from pions, neutrals, and the beamline were negligible, and are discussed in [15].

After all corrections, the elastic ^{27}Al asymmetry is

$$A_{\rm PV} = 2.16 \pm 0.11({\rm stat}) \pm 0.16({\rm syst}) \text{ ppm} \quad (5)$$

at $Q^2 = 0.02357 \pm 0.00010$ GeV^2, which corresponds to $\langle\theta_{\rm Lab}\rangle = 7.61^\circ \pm 0.02^\circ$. This result, the first on ^{27}Al, agrees well with previously published distorted wave Born calculations [9] as shown in Fig. 2.

The neutron distribution radius R_n was determined using a many-models correlation method first employed by the PREX collaboration [22]. A selection of relativistic mean-field models [23–29] were chosen based on their ability to reasonably predict several nuclear structure observables: nucleon binding energies, charge radii, and strengths of isoscalar and isovector giant resonances in selected nuclei. The relationship between R_n and A_{PV} was found to be

$$R_n = (-0.6007 \pm 0.0002)\frac{A_{\rm PV}}{\rm ppm} + (4.1817 \pm 0.0011) \text{ fm} \quad (6)$$

with correlation coefficient 0.997. Using this relation our final asymmetry yielded $R_n = 2.89 \pm 0.12$ fm, see Fig. 3.

To determine the neutron skin $R_n - R_p$, we use the pro-

TABLE II. Corrections applied to obtain the final asymmetry $A_{\rm PV}$ and their corresponding contributions to the systematic uncertainty. The total systematic uncertainty is the quadrature sum of these uncorrelated uncertainties.

Quantity	Value	$\Delta A_{\rm PV}/A_{\rm PV}$ (%)
$A_{\rm msr}$:	1.436 ± 0.014 ppm	1.0
P:	0.8880 ± 0.0055	0.7
$R_{\rm tot}$:	0.9855 ± 0.0087	0.9
$f_{\rm QE}$:	21.2 ± 2.9 %	5.0
$A_{\rm QE}$:	-0.34 ± 0.17 ppm	2.4
$f_{\rm nucl}$:	3.83 ± 0.23 %	0.1
$A_{\rm nucl}$:	2.58 ± 1.40 ppm	3.6
$f_{\rm inel}$:	0.665 ± 0.099 %	0.2
$A_{\rm inel}$:	-0.58 ± 5.83 ppm	2.6
$f_{\rm alloy}$:	5.41 ± 0.34 %	0.1
$A_{\rm alloy}$:	1.90 ± 0.58 ppm	2.1
$f_{\rm pions}$:	0.06 ± 0.06 %	0.1
$A_{\rm pions}$:	0 ± 20 ppm	0.8
$f_{\rm neutral}$:	0 ± 0.45 %	0.1
$A_{\rm neutral}$:	1.7 ± 0.2 ppm	0.0
$f_{\rm beamline}$:	0.69 ± 0.06 %	0.1
$f_{\rm GDR}$:	0.045 ± 0.023 %	0.1
$A_{\rm GDR}$:	-2.22 ± 1.11 ppm	0.0
Total Systematic		7.6

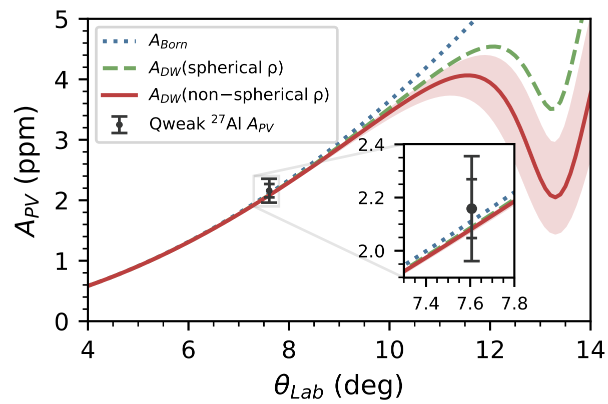

FIG. 2. Parity-violating asymmetry vs. laboratory scattering angle. The measured value is shown with statistical (inner error bar) and total (outer error bar) uncertainties. The theoretical prediction [9] at our beam energy is shown for spherically symmetric neutron and proton densities in Born approximation (blue dots), for a distorted wave calculation with spherical densities (dashed green line) and the full calculation with non-spherical proton density (red solid line). The red shaded band indicates nuclear structure and Coulomb distortion uncertainties.

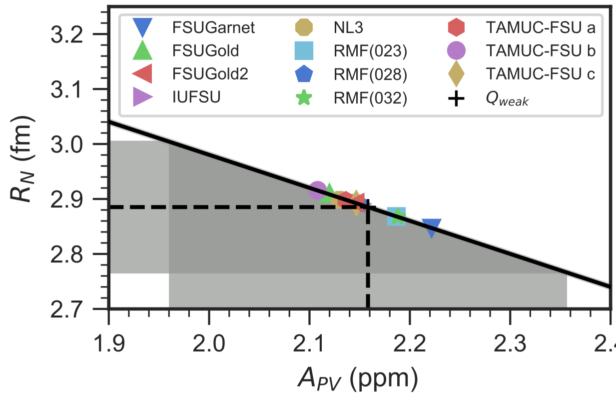

FIG. 3. Models (symbols indicated in the legend) used to establish the correlation (Eq. 6, and solid black line) between the ^{27}Al $A_{\rm PV}$ and its neutron radius R_n. The dashed black lines indicate where on the many-models correlation plot the central value of our asymmetry determines R_n. The shaded bands indicate the total uncertainty associated with our result.

ton distribution radius R_p following Ref. [30] for spherical nuclei,

$$R_p = \left(R_{\rm ch}^2 - \langle r_p^2\rangle - \frac{N}{Z}\langle r_n^2\rangle - \frac{3}{4m_N^2} - \langle r_{\rm so}^2\rangle\right)^{1/2} = 2.925 \pm 0.007 \text{ fm}, \tag{7}$$

where m_N is the nucleon mass, and N denotes the number of neutrons. Here and below we use an ^{27}Al charge radius $R_{\rm ch} = 3.035 \pm 0.002$ fm [31], and correct for the proton charge radius $\langle r_p\rangle = 0.8751 \pm 0.0061$ fm [32], the neutron charge radius $\langle r_n^2\rangle = -0.1161 \pm 0.0022$ fm^2 [13], and a spin-orbit nuclear charge correction $\langle r_{\rm so}^2\rangle = -0.017$ fm^2 following [30]. For consistency these parameters must be the same as those used to extract R_n using Eq. 6. The neutron skin is $R_n - R_p = -0.04 \pm 0.12$ fm, confirming the naive expectation for a light nucleus such as ^{27}Al where $N \approx Z$ that the neutron skin should be close to zero within our uncertainty. To illustrate the sensitivity of R_p to its input parameters, using other recent values for $\langle r_p\rangle$ [13] and $R_{\rm ch}$ [33] would only raise R_p by 1%, which is small compared to our 4.2% precision for R_n.

In order to proceed to estimates of electroweak (EW) observables to which this experiment is sensitive (see Tab. III), we follow the Born approximation (tree-level) formulation presented in [34]. Although this leads only to approximate EW results, the 9.1% precision of our asymmetry is large enough to blunt the need for a more precise treatment. In addition, Fig. 2 shows that the Born approximation accurately predicts our asymmetry. Moreover, the relatively low Z of ^{27}Al reduces the corrections from Coulomb distortions ($\propto Z$) relative to a heavier nucleus like Pb.

Following Ref. [34], we introduce a term Δ which accounts for hadronic and nuclear structure effects at $Q^2 > 0$:

$$\Delta \equiv \frac{F_{\rm wk}(Q^2)}{F_{\rm EM}(Q^2)} - 1 = \frac{A_{\rm PV}}{A_0}\frac{Z}{Q_W} - 1, \tag{8}$$

where $A_0 = -G_F Q^2/(4\pi\alpha\sqrt{2})$. Inserting our $A_{\rm PV}$ result (Eq. 5) into either Eq. 1 or Eq. 8, and using an $F_{\rm EM} = 0.384 \pm 0.012$ calculated following the prescription outlined in [35], we obtain a weak form factor $F_{\rm wk}(Q^2 = 0.0236\text{ GeV}^2) = 0.393 \pm 0.038$. The $F_{\rm EM}$ calculation (corrected for small Coulomb distortions) is good to about 3% [35], which we verified by comparing with differential cross section data [36].

With our $A_{\rm PV}$ result, $\Delta = 0.025 \pm 0.094$. To lowest order in Q^2, $R_{\rm wskin} \equiv R_{\rm wk} - R_{\rm ch} = -3\Delta/(Q^2 R_{\rm ch})$ [34], from which we obtain $R_{\rm wskin} = -0.04 \pm 0.15$ fm, consistent as expected with our small neutron skin result. Employing the $R_{\rm ch}$ introduced earlier, $R_{\rm wk} = 3.00 \pm 0.15$ fm. The relative difference between the weak and charge radii $\lambda \equiv (R_{\rm wk} - R_{\rm ch})/R_{\rm ch} = -1.3\% \pm 5.0\%$.

TABLE III. Derived ^{27}Al Observables

Observable	Value	Uncertainty	Units
R_n	2.89	0.12	fm
$R_n - R_p$	-0.04	0.12	fm
$F_{\rm wk}(Q^2 = 0.0236\text{ GeV}^2)$	0.393	0.038	
$\Delta = ZA_{\rm PV}/(A_0 Q_W) - 1$	0.025	0.094	
$R_{\rm wskin} = -3\Delta/(Q^2 R_{\rm ch})$	-0.04	0.15	fm
$R_{\rm wk} = R_{\rm wskin} + R_{\rm ch}$	3.00	0.15	fm
$\lambda \equiv (R_{\rm wk} - R_{\rm ch})/R_{\rm ch}$	-1.3	5.0	%

In conclusion, the agreement between predictions [9] and this first measurement of the elastic asymmetry on ^{27}Al supports the background procedures used in the $Q_{\rm weak}$ experiment [4] on hydrogen. The tree-level EW results obtained above for $R_{\rm wk}$ and $R_{\rm wskin}$ are consistent with broad expectations for a low-Z nucleus with $N \approx Z$ such as ^{27}Al. Similarly, our ^{27}Al neutron skin is close to zero, as expected, providing some validation and a benchmark for the application of the many-models approach and EW technique [10] to the measurement of heavier nuclei [5, 6, 22].

This is especially interesting in light of the tension which exists [11, 37–39] between the recent EW neutron skin determination $R_n - R_p = 0.283 \pm 0.071$ fm for ^{208}Pb [5], and the 2012 average of several disparate but self-consistent non-EW determinations $R_n - R_p = 0.184 \pm 0.027$ fm [12]. The older non-EW determinations have come under additional scrutiny and even some criticism recently [40]. However, we note that they appear to be more consistent with the latest constraints on neutron star properties from LIGO and Virgo (especially for the tidal deformability) [41], from NICER [7], and astrophysical models in general.

We thank the staff of Jefferson Lab, in particular the accelerator operations staff, the radiation control staff, as well as the Hall C technical staff for their help and support. We are also grateful for the contributions of our undergraduate students. We thank TRIUMF for its contributions to the development of the spectrometer and integrated electronics, and BATES for its contributions to the spectrometer and Compton polarimeter. We also thank T.W. Donnelly for helpful discussions. This material is based upon work supported by the U.S. Department of Energy (DOE), Office of Science, Office of Nuclear Physics under contract DE-AC05-06OR23177. Construction and operating funding for the experiment was provided through the DOE, the Natural Sciences and Engineering Research Council of Canada (NSERC), the Canada Foundation for Innovation (CFI), and the National Science Foundation (NSF) with university matching contributions from William & Mary, Virginia Tech, George Washington University and Louisiana Tech University.

* corresponding author: armd@physics.wm.edu
† Deceased
‡ corresponding author: smithg@jlab.org
§ Now at Manhattan College, Riverdale, New York 10471, USA
¶ Now at University of Tennessee, Knoxville, Tennessee 37796, USA

[1] P. Souder, J. Bellanca, G. Cates, G. Dodson, K. Dow, M. Farkhondeh, R. Holmes, V. Hughes, T. Gay, K. Isakovich, et al., Nucl. Phys. A **527**, 695 (1991).
[2] D. S. Armstrong and R. D. McKeown, Ann. Rev. Nucl. Part. Sci. **62**, 337 (2012).
[3] D. Androić, D. S. Armstrong, A. Asaturyan, T. Averett, J. Balewski, J. Beaufait, R. S. Beminiwattha, J. Benesch, F. Benmokhtar, J. Birchall, et al. (Q_{weak} Collaboration), Phys. Rev. Lett. **111**, 141803 (2013), URL https://link.aps.org/doi/10.1103/PhysRevLett.111.141803.
[4] D. Androić et al. (Q_{weak} Collaboration), Nature **557**, 207 (2018).
[5] D. Adhikari et al. (PREX), Phys. Rev. Lett. **126**, 172502 (2021).
[6] C. J. Horowitz, K. S. Kumar, and R. Michaels, Eur. Phys. J. A **50**, 48 (2014).
[7] B. T. Reed, F. J. Fattoyev, C. J. Horowitz, and J. Piekarewicz, Phys. Rev. Lett. **126**, 172503 (2021), URL https://link.aps.org/doi/10.1103/PhysRevLett.126.172503.
[8] R. D. Carlini, W. T. H. van Oers, M. L. Pitt, and G. R. Smith, Ann. Rev. Nucl. Part. Sci. **69**, 191 (2019).
[9] C. J. Horowitz, Phys. Rev. C **89**, 045503 (2014), URL https://link.aps.org/doi/10.1103/PhysRevC.89.045503.
[10] C. J. Horowitz, S. J. Pollock, P. A. Souder, and R. Michaels, Phys. Rev. C **63**, 025501 (2001), URL https://link.aps.org/doi/10.1103/PhysRevC.63.025501.
[11] J. Piekarewicz, Phys. Rev. C **104**, 024329 (2021), URL https://link.aps.org/doi/10.1103/PhysRevC.104.024329.
[12] M. B. Tsang et al., Phys. Rev. **C86**, 015803 (2012).
[13] P. Zyla et al. (Particle Data Group), PTEP **2020**, 083C01 (2020).
[14] T. Allison, M. Anderson, D. Androić, D. Armstrong, A. Asaturyan, T. Averett, R. Averill, J. Balewski, J. Beaufait, R. Beminiwattha, et al. (Q_{weak} Collaboration), Nucl. Instrum. Methods **A781**, 105 (2015), ISSN 0168-9002, URL http://www.sciencedirect.com/science/article/pii/S0168900215000509.
[15] K. D. Bartlett, Ph.D. thesis, College of William & Mary (2018), URL https://doi.org/10.2172/1468743.
[16] W. Duvall, Ph.D. thesis, Virginia Polytechnic Institute and State University (2017), URL https://misportal.jlab.org/ul/publications/downloadFile.cfm?pub_id=15805.
[17] D. Androić et al. (Q_{Weak}), Phys. Rev. C **104**, 014606 (2021), 2103.09758, URL https://link.aps.org/doi/10.1103/PhysRevC.104.014606.
[18] A. Narayan et al., Phys. Rev. X **6**, 011013 (2016).
[19] M. Hauger et al., Nucl Inst.& Meth. A **462**, 382 (2001).
[20] J. Magee, A. Narayan, D. Jones, R. Beminiwattha, J. Cornejo, M. Dalton, W. Deconinck, D. Dutta, D. Gaskell, J. Martin, et al., Physics Letters B **766**, 339 (2017), ISSN 0370-2693, URL https://www.sciencedirect.com/science/article/pii/S0370269317300333.
[21] C. J. Horowitz and J. Piekarewicz, Phys. Rev. **C47**, 2924 (1993).
[22] S. Abrahamyan, Z. Ahmed, H. Albataineh, K. Aniol, D. S. Armstrong, W. Armstrong, T. Averett, B. Babineau, A. Barbieri, V. Bellini, et al. (PREX Collaboration), Phys. Rev. Lett. **108**, 112502 (2012), URL https://link.aps.org/doi/10.1103/PhysRevLett.108.112502.
[23] B. G. Todd-Rutel and J. Piekarewicz, Physical Review Letters **95**, 122501 (2005), URL https://link.aps.org/doi/10.1103/PhysRevLett.95.122501.
[24] W.-C. Chen and J. Piekarewicz, Physical Review C **90**, 044305 (2014), URL https://link.aps.org/doi/10.1103/PhysRevC.90.044305.
[25] G. A. Lalazissis, J. König, and P. Ring, Physical Review C **55**, 540 (1997), URL https://link.aps.org/doi/10.1103/PhysRevC.55.540.
[26] G. Lalazissis, S. Raman, and P. Ring, Atomic Data and Nuclear Data Tables **71**, 1 (1999), ISSN 0092-640X, URL http://www.sciencedirect.com/science/article/pii/S0092640X98907951.
[27] F. J. Fattoyev, C. J. Horowitz, J. Piekarewicz, and G. Shen, Physical Review C **82**, 055803 (2010), URL https://link.aps.org/doi/10.1103/PhysRevC.82.055803.
[28] F. J. Fattoyev and J. Piekarewicz, Physical Review Letters **111**, 162501 (2013), URL https://link.aps.org/doi/10.1103/PhysRevLett.111.162501.
[29] W.-C. Chen and J. Piekarewicz, Physics Letters B **748**, 284 (2015), ISSN 0370-2693, URL http://www.sciencedirect.com/science/article/pii/S0370269315005304.
[30] A. Ong, J. C. Berengut, and V. V. Flambaum, Phys. Rev. C **82**, 014320 (2010).
[31] C. D. V. H. De Vries, C.W. De Jager, Atomic Data and Nuclear Data Tables **36**, 495 (1987), ISSN 0092-640X, URL https://www.sciencedirect.com/science/article/pii/0092640X87900131.

[32] C. Patrignani et al. (Particle Data Group), Chin. Phys. C **40**, 100001 (2016 and 2017 update).
[33] H. Heylen, C. S. Devlin, W. Gins, M. L. Bissell, K. Blaum, B. Cheal, L. Filippin, R. F. G. Ruiz, M. Godefroid, C. Gorges, et al., Phys. Rev. C **103**, 014318 (2021), URL https://link.aps.org/doi/10.1103/PhysRevC.103.014318.
[34] O. Koshchii, J. Erler, M. Gorchtein, C. J. Horowitz, J. Piekarewicz, X. Roca-Maza, C.-Y. Seng, and H. Spiesberger, Phys. Rev. C **102**, 022501(R) (2020), URL https://doi.org/10.1103/PhysRevC.102.022501.
[35] T. Stovall, D. Vinciguerra, and M. Bernheim, Nuclear Physics A **91**, 513 (1967), ISSN 0375-9474, URL https://www.sciencedirect.com/science/article/pii/0375947467905714.
[36] G. C. Li, M. R. Yearian, and I. Sick, Phys. Rev. C **9**, 1861 (1974), URL https://link.aps.org/doi/10.1103/PhysRevC.9.1861.
[37] P.-G. Reinhard, X. Roca-Maza, and W. Nazarewicz, Phys. Rev. Lett. **127**, 232501 (2021), URL https://link.aps.org/doi/10.1103/PhysRevLett.127.232501.
[38] R. Essick, P. Landry, A. Schwenk, and I. Tews, Phys. Rev. C **104**, 065804 (2021), URL https://link.aps.org/doi/10.1103/PhysRevC.104.065804.
[39] E. R. Most and C. A. Raithel (2021), arXiv:2107.06804.
[40] M. Thiel, C. Sfienti, J. Piekarewicz, C. J. Horowitz, and M. Vanderhaeghen, Journal of Physics G: Nuclear and Particle Physics **46**, 093003 (2019).
[41] B. P. Abbott, R. Abbott, T. D. Abbott, F. Acernese, K. Ackley, C. Adams, T. Adams, P. Addesso, R. X. Adhikari, V. B. Adya, et al. (The LIGO Scientific Collaboration and the Virgo Collaboration), Phys. Rev. Lett. **121**, 161101 (2018), URL https://link.aps.org/doi/10.1103/PhysRevLett.121.161101.